EFFECTS OF HEAT TREATMENT ON TENSILE PROPERTIES OF 3D-PRINTED SHORT FIBER-REINFORCED COMPOSITES

AUTHORS:
A. Shuaibu[1,*], and A. Ahmad[2]

AFFILIATIONS:
[1]School of Traffic and Transportation, Engineering, Central South University, Changsha 410075, China.
[2]Department of Civil Engineering, Ahmadu Bello University, Zaria 810107, Nigeria

*CORRESPONDING AUTHOR:
Email: abdusule97@gmail.com

Abstract

3D-printed carbon fibre-reinforced composites (CFRC) using fused deposition modelling (FDM) offer the potential for building complex geometries and low waste. However, these composites have weaker interlaminar bonding and higher void content than traditional composites. This paper explores the effect of temperature on improving the mechanical properties of 3D-printed short carbon fibre-reinforced polyamide (PACF). Two types of printed structures were tested: one with a 0° build orientation (parallel to extruder movement) and the other with a 90° build orientation (perpendicular to extruder movement). Both samples were heat-treated at 150°C. Force vs. displacement data was obtained from the MTS testing machine. After that, the tested samples were viewed under an optical microscope. Images obtained from the optical microscope are then analyzed to see how the samples failed by checking the microstructure. The average ultimate strength, ultimate strain, and elastic modulus were used for the analysis. The sample follows a trend where the strength and elastic modulus increase after heat treatment. The result also showed that the 0° build orientation samples have higher mechanical performance than the 90° build orientation sample. Also, from the ultimate strain values, it was evident that samples printed in the 0° absorbed more energy, exhibiting 83% higher resistance before final failure. Lastly, an optical microscope was used to investigate the failure mechanisms of the samples.

1.0 INTRODUCTION

Engineers are known to design different types of parts. A consideration in designing those parts is the technique to manufacture them. There are many methods by which the parts can be manufactured, each with strengths and limitations. Generally, a 3D part or object can be produced through forming, additive, and subtractive manufacturing. In forming, the workpieces are primarily metals. They are usually mechanically deformed and reshaped by applying heat or pressure without adding or subtracting materials, for example, injection moulding, casting, and forging. In subtractive manufacturing, the unwanted materials are removed from the workpiece until the desired or needed shape is achieved. This includes processes like turning, milling, and drilling. The last method is additive manufacturing (AM), known as 3D printing, where materials are deposited layer after layer sequentially to form the required 3D virtual model [1].

Carbon fibre-reinforced polymer composites (CFRP) play a crucial role in aerospace, energy, and

automotive industries, where weight reduction is vital. The exploration of additively manufactured (AM) fibre-reinforced polymer composites (FRP) is relatively new but offers distinct advantages over conventional methods [2], [3]. Additive manufactureng of composites can eliminate moulds, enable intricate shapes, and optimize fibre alignment for better weight-specific mechanical properties [4]. Polymer and reinforcement selection hinges on application, manufacturing ease, and cost. Carbon fibre advantages in additive manufacturing, include enhanced thermal conductivity, stiffness, and minimized thermal expansion, facilitating larger builds with tighter precision [3]. In comparison, the longitudinal mechanical properties of 3D-printed FRP match those of traditionally fabricated composites [5], [6].

The inherent defects resulting from the fused deposition modelling method significantly impact both transverse and interlaminar responses (normal and shear). These defects are attributed to inadequate thermomechanical consolidation during material deposition [7]. Various factors like layer thickness [8], fibre volume [8], printing parameters [9] and trajectories [10] influence the performance of 3D-printed carbon, glass, and Kevlar composites. Moreover, the properties of commercially available printable materials in this technology impede proper layer adhesion, in contrast to other common thermoplastics used in fused filament fabrication (FFF) technology, and the inhomogeneous fibre distribution in the microstructure may cause premature failure [11]. These observations highlight the need for a comprehensive strategy to make 3D printing of CFRP a feasible method for producing high-performance structural components [7], [12], [13].

Enhancing the mechanical characteristics of AM components is often accomplished by optimizing print parameters, including printing speed, layer height, and chamber, bed, and extrusion temperatures, along with post-processing thermal treatments [1], [14], [15]. The prevalent mechanisms associated with enhancing mechanical properties in AM polymers and composites involve void reduction, mitigation of residual thermal stresses, and elevation of polymer crystallinity [15], [16]. Post-processing, including heat and chemical treatments, can significantly influence the mechanical properties of the structure. Pascual-Gonzalez et al. [17] studied 3D-printed carbon fibre composites and found that post-processing at 150°C improved microstructure, moisture content, void content, dimensional accuracy,

and thermal and mechanical properties. The porosity decreased by 87%, and interlaminar strength increased by 145%. De Avila et al. [18] observed an increased strength through heat treatment, driven by material re-crystallization, cautioning against surpassing the glass transition temperature (T_g) to avoid brittleness. Guduru and Srinivasu [19] investigated chemical and heat treatment on carbon-infused polylactic acid (PLA) composite and found that chemical treatment increased tensile properties by 12%, while heat treatment only increased by 6%. Meng et al. [20] investigated the annealing effects on the mechanical properties and the crystalline structure of polyamide 66 reinforced with 50 wt.% glass fibre. They found that the material's tensile strength, Young modulus, and flexural properties increased from 10% to 30% at all annealing temperatures. Still, there was a loss in impact strength, ductility, and toughness. In another study by Ivey et al. [21], annealing improved the printed layers, but the study did not significantly improve mechanical properties. The samples were annealed above the T_g. Shiao et al. [22] [23] surveyed annealing's effects on glass-fiber-reinforced nylon 6,6 (GFRP).

Additionally, achieving a critical fibre volume enhanced localized plasticity, and fracture toughness was improved through annealing. El Magri et al. [24] investigated annealing's impact on PLA and carbon fiber-reinforced PLA. Carbon-reinforced PLA consistently had a higher tensile modulus than pure PLA after annealing. A slower cooling rate enhanced the samples' crystallinity and Young's modulus. Bhandari et al. [25] improved the interlayer strength of carbon fiber-PLA and PETG composites through annealing, enhancing properties like tensile strength and ductility. Hoang et al. [26] compared annealing, vacuum bag only (VBO), and hot pressing for carbon-Polyetherketoneketone composites; hot pressing yielded the least voids, highest strength, and crystallinity. Geng et al. [27] improved 3D-printed PPS part strength via heat treatment, but impact resistance decreased due to higher elasticity.

This study aims to investigate the effect of heat treatment on the mechanical properties of 3D-printed short carbon fibre-reinforced polyamide (PACF). Samples were printed using the FDM technique. The effect of build orientation and the failure mechanisms concerning different conditions are also investigated.

2.0   EXPERIMENTAL METHOD
2.1   Material
The material used in this experiment is short carbon fibre-reinforced polyamide (PACF) with a filament

diameter of 1.75 mm, bought from eSUN (Shenzhen, China). It has a melting temperature of 250°C. The PACF filament comprises 74% polyamide (PA), 25% carbon fibre, and 1% additives. Material properties of the filaments are provided in the Table 1.

Table 1: Material properties of PACF

Material Properties	PACF
Density (g/cm³)	1.24
Tensile Strength (MPa)	75
Elongation (%)	26
Flexural Strength (MPa)	122

2.2 3D Printer and Slicing Software

The test samples were manufactured using a Raise3D Pro2 Series 3D printer utilizing the FDM technique. This printer can print various filaments at temperatures of up to 300°C. Additionally, the printer boasts an exceptional visual interface, allowing for quick review and monitoring of the printing progress. Before printing, the STL files obtained from computer-aided design software were preprocessed in a slicing software called ideaMaker. This slicer software divides the STL file into printable layers and converts the model from STL format into g-code instructions, the instructions the printer understands.

2.3 Test Samples Preparation

Hollow triangular prisms with a thin wall thickness of 1.9 mm were 3D-printed using the parameters outlined in Table 2.
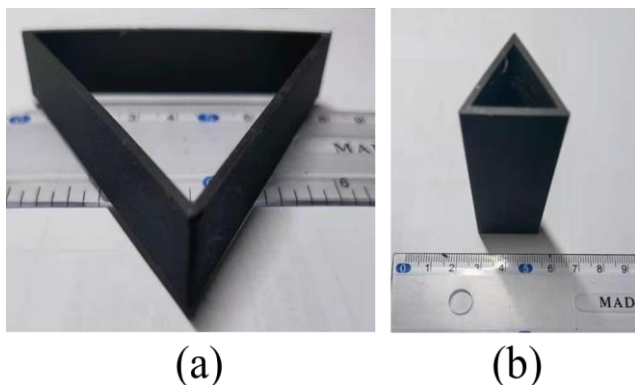
Figure 1: 3D-printed structures samples (a) 0° build orientation (b) 90° build orientation

Table 1: Printing parameters used in 3D-printed samples

Parameter	Value
Layer thickness	0.15 mm
Infill density	100 %
Printing speed	60 mm/s
Printing temperature	240°C
Printing bed temperature	70°C

After printing, the samples (Figure 1) undergo heat treatment and are cut into ASTM D638 type IV standard tensile test samples (Figure 2c). The walls of the triangular prism are machined using a cutter, yielding three tensile samples from each prism. This approach was chosen to ensure dimensional stability and enhance the interlaminar strength of the test samples. Two types of samples are machined from the structures shown in Figure 1. The first type has the sample length parallel to the extruder movement direction, aligned with the X-Y plane (0° build orientation, Figure 2a). The second type has the sample length perpendicular to the extruder movement direction, oriented in the Z-direction (90° build orientation, Figure 2b). This way of printing the tensile test samples is preferred due to their thin and slender nature, making it challenging to print them upright. It also reduces the impact of heating from the printer bed platform.
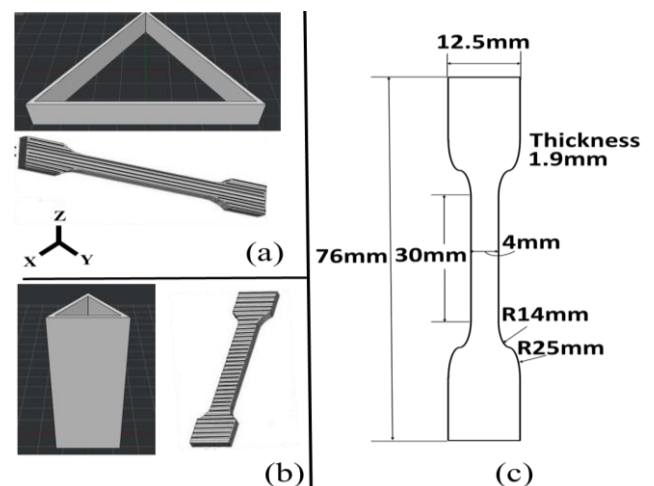
Figure 2: A sketch of the printed structures and tensile samples (a) 0° build orientation (b) 90° build orientation. (c) Test sample dimensions

Figure 3: Air oven used for heat treatment

2.4 Heat Treatment

The printed structures were subjected to different post-treatment times and temperatures. So, for each type of build orientation, three structures were machined. Table 3 provides details on the time and temperature to which the structures were exposed.

Table 2: Material samples and their corresponding heat treatment time and temperatures

Structure	T (°C)	Time (h)
0°	T (amb)	0
	150	2
90°	T (amb)	0
	150	2

The heat treatment was performed in a closed-air oven (Figure 3). The oven was preheated at 150°C before the structures were inserted. Once the heat treatment was completed, the oven was turned off. The structures were only removed after cooling to room temperature to prevent warping. The tensile test samples were then cut from the structures, 3 from each structure (see Figure 2). Heat treatment processes are employed in polymer manufacturing to enhance material strength. Polymer composites have already shown improved strength after heat treatment. This method enhances the properties of 3D-printed samples by evenly distributing stresses, increasing tensile strength, and reducing the likelihood of quick or easy fracture [28]. As supported by relevant literature, the treatment temperature of 150 °C was based on considerations such as precision of final part measurements, microstructure, thermal, and mechanical properties [17].

2.5 Tensile Test

Post-treatment effects on samples were examined through a tensile test using the MTS exceed model E44 universal testing machine (Figure 4a). Fixtures attached to the machine were used to vertically position the dog bone samples. The testing machine has a maximum force capacity of 30kN with a maximum and minimum test speed of 500 mm/min and 0.001 mm/min. The top head of the fixture moves under continuous tensile load until the material fails. Data, including applied force, displacement, stress, and strain values, is recorded using the TestSuite TW software. Elastic modulus values for each sample set are then determined and documented. The results are imported into MS Excel for analysis and visualized through a bar chart comparing stress, strain, and elastic modulus values.

2.6 Microscopy Study on Tested Samples

This procedure was performed using an optical microscope (AO-3M150GS, AOSVI, Shenzhen, China), as shown in Figure 4b. Images obtained from

the optical microscope are then analyzed. This was done to see how the samples failed by checking the microstructure.
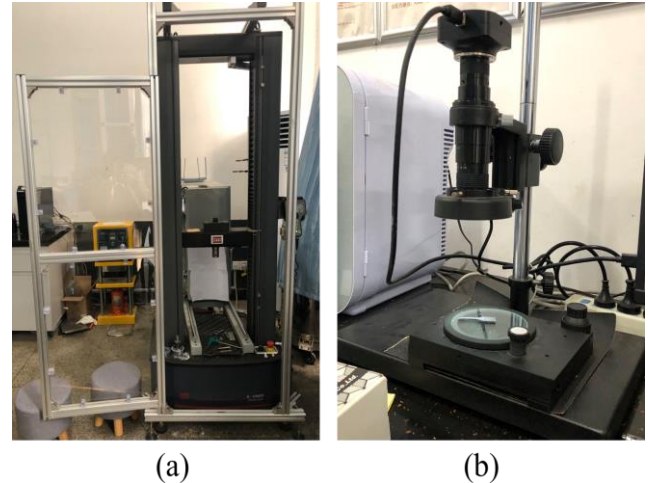
Figure 4: (a) MTS universal testing machine used for tensile testing (b) Optical Microscope

3.0 RESULTS AND DISCUSSION
3.1 Tensile Test Results
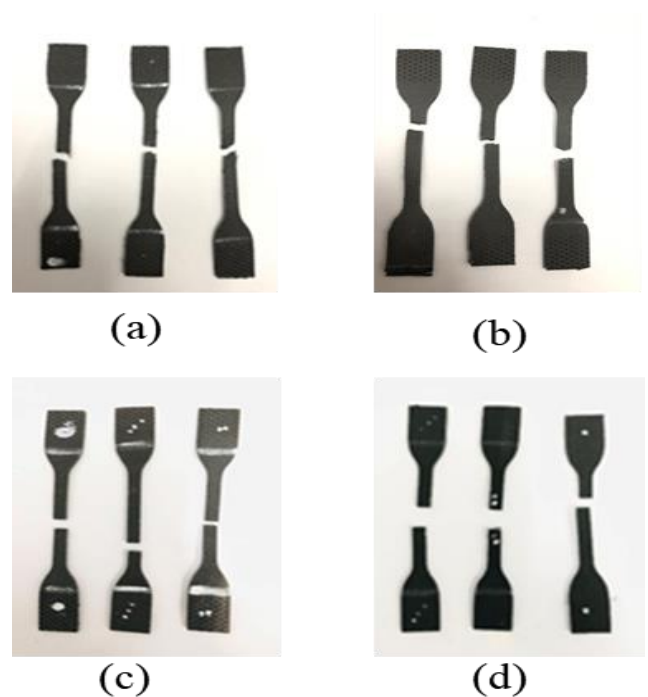
Figure 5: Tested samples (a) Untreated 0° build (b) Heat-treated 0° build (c) Untreated 90° build (d) Heat-treated 90° build

Figure 5 shows all the tested samples. The stress vs. strain plots for the PACF samples, tested under different conditions, are shown in Figure 6. These plots showcase the results obtained from twelve (12) samples tested at room temperature. Six of the twelve samples were obtained from the Z-direction-aligned sample (90° build orientation), while the other six

were obtained from the X-Y plane-aligned sample (0° build orientation). The results and the average values for the elastic modulus, ultimate tensile strength, and ultimate strain are shown in Tables 4 and 5. The elastic modulus was determined by taking the slope of the linear segment of the curve, and the average values were subsequently compared.
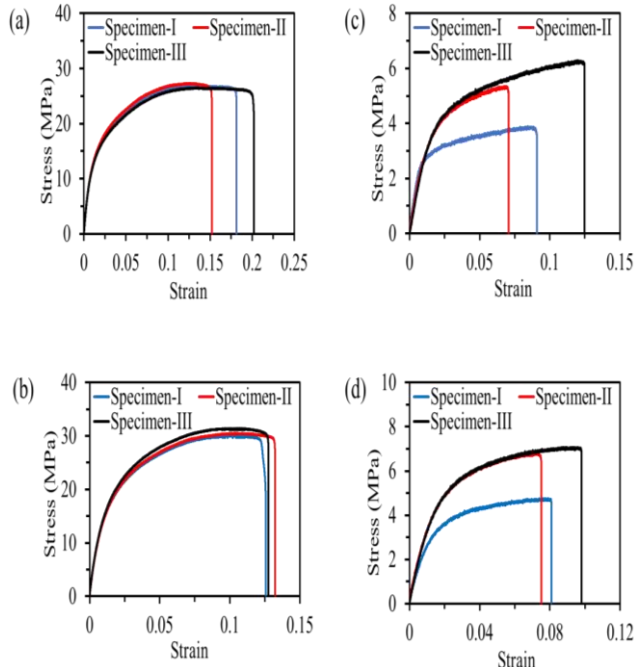
Figure 6: The stress-strain plot of the tested samples (a) Untreated 0° build (b) Heat-treated 0° build (c) Untreated 90° build (d) Heat-treated 90° build.

Table 4: Tensile test result of untreated samples

Build orientation	Sample	Elastic modulus (MPa)	Ultimate strength (MPa)	Ultimate strain
0° build orientation samples	I	1686.30	26.92	0.1814
	II	1707.40	27.32	0.1521
	III	1671.90	26.50	0.2021
	Average	1688.53	26.91	0.1785
90° build orientation samples	*I	390.00	3.88	0.0909
	II	314.55	5.35	0.0707
	III	278.95	6.29	0.1249
	Average	296.75	5.82	0.0978

Table 5: Tensile test result of heat-treated samples

Build orientation	Sample	Elastic modulus (MPa)	Ultimate strength (MPa)	Ultimate strain
0° build orientation samples	I	1994.00	29.99	0.1258
	II	1993.60	30.49	0.1323
	III	2111.10	31.40	0.1275
	Average	2032.80	30.63	0.1285
90° build orientation samples	*I	356.57	4.76	0.0809
	II	412.74	6.81	0.0752
	III	401.39	7.42	0.0981
	Average	407.07	7.12	0.0867
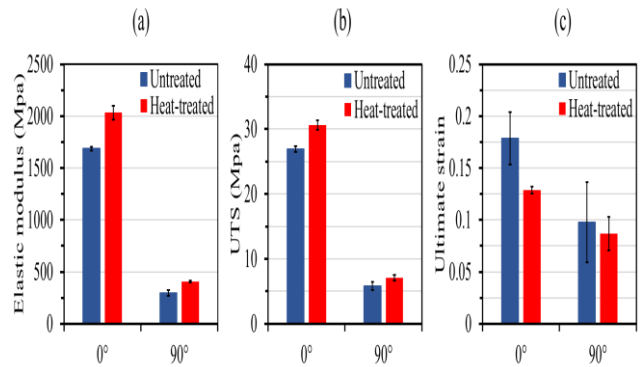
Figure 7: Comparison of measured Mechanical properties for PACF samples in untreated and heat-treated conditions, (a) elastic modulus, (b) ultimate tensile strength, (c) ultimate strain

3.2 Effect of Heat Treatment Temperature

Figure 6 shows the stress-strain plot of the untreated and heat-treated samples. It is evident from this figure that the post-heat-treatment temperature caused the sample to fail at a relatively lower strain. Nevertheless, there was an increase in the tensile strength of the PACF sample in both build orientations. The average tensile strength of the untreated 0° PACF sample was 26.91 MPa. Heat treating the sample at 150°C increased the tensile strength by 14%. The modulus of elasticity also increased by 20% for heat-treated samples. Enhanced interfacial bonding between carbon fibres and the polyamide matrix. As the temperature rises, the polymer chains become more flexible, allowing for better wetting and dispersion of the glass fibres within the matrix. This improved bonding results in a stronger and more uniform microstructure, which translates to enhanced mechanical performance. Also, increased temperature can partially melt the nylon matrix, allowing for better compaction and filling of void spaces between the deposited filaments.

This compaction reduces the air gaps and discontinuities that can act as stress concentration points, further improving the overall mechanical integrity of the composite [28]. Changing the build orientation to 90° significantly decreased the tensile strength of the samples. The tensile strength of the untreated 90° PACF sample was 5.82 MPa. Heat treating the sample increased the tensile strength by 22%. An increase is also seen in the elastic moduli by 37% for heat-treated samples. It was observed that following heat treatment, the tested samples showed negligible or no change in their dimensions, warping, or curling. The temperature has been instrumental in enhancing both the tensile strength and elastic modulus of the sample. This was attributed to the temperature, causing the layers to adhere better.

Figure 7 compares the average values of the mechanical properties of the PACF samples.

3.3 Effect of Build Orientation

Testing the sample with sample length in the Z-direction, that is, the 90° build orientation sample, is to test the adhesive strength between the layers. It can be seen that the 90° samples have the lowest ultimate tensile strength, elastic modulus, and strain. The tensile strength of the untreated and heat-treated 90° samples was 5.82 MPa and 7.12 MPa, respectively, while for the 0° sample, it was 26.91 MPa and 30.63 MPa, respectively. As seen, there is an increase of about 362% and 330% in tensile strength of the untreated and heat-treated samples, respectively, when compared to the 0° samples. Also, looking at the elastic moduli values in Figure 7, there was an increase of about 469% and 399% in the elastic moduli of the untreated and heat-treated samples, respectively, compared to the 0° samples. For the elastic strain, it is evident that samples printed in the 0° absorbed more energy, exhibiting higher plastic deformation and toughness before final failure. As initially reviewed, one critical factor that impacts the printed samples' mechanical properties is build orientation or raster angle. The significant difference in tensile strength is due to the perpendicular nature of the layers to the direction of the tensile force. In other words, the 90° samples fail at the interlayer bond between the beads, while much more force is required to fracture the filament in the 0° samples. This explains why the 0° sample has higher tensile strength.

3.4 Microscopy Imaging Analysis

Analyzing the tested samples' failure modes using an optical microscope helps better understand the microstructural failure mechanisms of the samples. The analysis indicated the presence of voids in both the PACF filament and the printed samples. This may be caused by air bubble formation during carbon fibre addition in the PA matrix during filament production. Voids in printed PACF samples may result from extruder clogging or weak bonding between layers. The reduction or complete elimination of these voids should enhance the mechanical properties of the printed sample. At a molecular level, achieving robust chemical bonding between the polymer chains within adjacent beads is essential for effective load transfer, ensuring the production of a high-strength component. Figure 8 shows the microscopy image of the samples. As seen, the untreated samples tend to have more voids than the heat-treated samples, as one layer was not fully integrated into the others. It shows the spaces between them. The samples heat-treated tend to have a more compact structure. It is noticeable from Figures

8a and 8b that the samples exhibited ductile fracture. It clearly shows that the sample materials flow before fracture. It can also be seen from the images obtained from the microscope in Figures 8c and 8d that it is a brittle fracture because the fractured surface looks smooth. Also, the small elongation to fracture was noticed throughout the testing period.
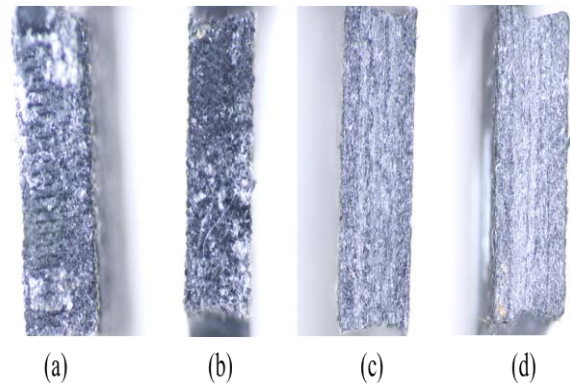
Figure 7: Optical microscopy of the cross-sectional images of tensile test samples showing fracture surfaces (a) Untreated 0° build (b) Heat-treated 0° build (c) Untreated 90° build (d) Heat-treated 90° build

4.0 CONCLUSION

The required dimensions for the polyamide carbon fibre (PACF) composite sample were obtained using 3D printing. This paper studied the mechanical properties and failure morphologies of PACF 3D-printed samples following post-printing heat treatment. Tensile strength, elastic modulus, and ultimate tension at break are parameters used to assess the structures. After heat treatment, 0^0 build samples showed a 20% increase in elastic modulus, a 14% increase in ultimate tensile strength, and a 28% decrease in ultimate strain, while 90^0 build samples showed a 37% increase in elastic modulus, a 22% increase in ultimate tensile strength, and an 11% decrease in ultimate strain. Heat treatment improved the mechanical properties of the samples. It also seemed to strengthen the interlayer bond. There were no signs of warping due to heat treatment in the treated samples in this experiment.

The 3D-printed samples' elastic modulus and ductility were improved after heat treatment. It's noteworthy that the 3D-printed samples exhibit visible anisotropic behaviour. When the printing orientation is the same as the sample length (0° build orientation), the samples have greater strength and elastic modulus than when the printing direction is 90° build orientation. The heat-treated 0° build orientation sample has the maximum average elastic modulus and ultimate tensile strength of 2032.80 MPa

and 30.63 MPa, respectively, according to the tensile test data. The untreated 0° built sample, on the other hand, has the largest ultimate strain at break (0.1785). While the optical microscope was helpful in the experiment, it did not provide enough detail to draw any conclusions about how or why the samples were stronger during post-treatment. However, another microstructural tool, such as scanning electron microscopy (SEM), may be used to learn more about the material's failure mechanism. To profit from polyamide's void closure and ductile characteristics, a multi-step post-processing strategy that includes heating under pressure followed by quenching might be explored.

REFERENCES

[1] Redwood, B., Schoffer, F., and Garret, B. "The 3D Printing Handbook Technologies, design, and applications", *3D Hubs B.V*, 2017.

[2] Brenken, B., Barocio, E., Favaloro, A., Kunc, V., and Pipes, R. B. "Fused filament fabrication of fiber-reinforced polymers: A review", *Addit Manuf*, vol. 21, pp. 1–16, May 2018, doi: 10.1016/j.addma.2018.01.002.

[3] van de Werken, N., Tekinalp, N., Khanbolouki, P., Ozcan, S., Williams, A., and Tehrani, M. "Additively manufactured carbon fiber-reinforced composites: State of the art and perspective", *Addit Manuf*, vol. 31, pp. 1–19, Jan. 2020, doi: 10.1016/j.addma.2019.100962.

[4] van de Werken, N., Hurley, J., Khanbolouki, P., Sarvestani, A. N., Tamijani, A. Y., and Tehrani, M. "Design considerations and modelling of fibre reinforced 3D printed parts", *Compos B Eng*, vol. 160, pp. 684–692, Mar. 2019, doi: 10.1016/j.compositesb.2018.12.094.

[5] Ma, Y., Ueda, M., Yokozeki, T., Sugahara, T., Yang, Y., and Hamada, H. "A comparative study of the mechanical properties and failure behaviour of carbon fibre/epoxy and carbon fibre/polyamide 6 unidirectional composites", *Compos Struct*, vol. 160, pp. 89–99, Jan. 2017, doi: 10.1016/j.compstruct.2016.10.037.

[6] Serna Moreno, M. C., Romero Gutiérrez, A., and Martínez Vicente, J. L. "Different response under tension and compression of unidirectional carbon fibre laminates in a three-point bending test", *Compos Struct*, vol. 136, pp. 706–711, Feb. 2016, doi: 10.1016/j.compstruct.2015.06.017.

[7] Iragi, M., Pascual-González, C., Esnaola, A., Lopes, C. S., and Aretxabaleta, L. "Ply and interlaminar behaviours of 3D printed continuous carbon fibre-reinforced thermoplastic laminates; effects of processing conditions and microstructure", *Addit Manuf*, vol. 30, pp. 1–12, Dec. 2019, doi: 10.1016/j.addma.2019.100884.

[8] Caminero, M. A., Chacón, J. M., García-Moreno, I., and Reverte, J. M. "Interlaminar bonding performance of 3D printed continuous fibre reinforced thermoplastic composites using fused deposition modelling", *Polym Test*, vol. 68, pp. 415–423, Jul. 2018, doi: 10.1016/j.polymertesting.2018.04.038.

[9] Li, H., Wang, T., Sun, J., and Yu, Z. "The effect of process parameters in fused deposition modelling on bonding degree and mechanical properties", *Rapid Prototyp J*, vol. 24, no. 1, pp. 80–92, 2018, doi: 10.1108/RPJ-06-2016-0090.

[10] Wang, S., Ma, Y., Deng, Z., Zhang, S., and Cai, J. "Effects of fused deposition modelling process parameters on tensile, dynamic mechanical properties of 3D printed polylactic acid materials", *Polym Test*, vol. 86, Jun. 2020, doi: 10.1016/j.polymertesting.2020.106483.

[11] Pascual-González, C., Iragi, M., Fernández, A., Fernández-Blázquez, J. P., Aretxabaleta, L., and Lopes, C. S. "An approach to analyse the factors behind the micromechanical response of 3D-printed composites", *Compos B Eng*, vol. 186, Apr. 2020, doi: 10.1016/j.compositesb.2020.107820.

[12] Soete, J., Badoux, B., Swolfs, Y., Gorbatikh, L., and Wevers, M. "Defect detection in 3D printed carbon fibre composites using X-ray Computed Tomography", *e-Journal of Nondestructive Testing*, vol. 24, no. 3, Mar. 2019, doi: 10.58286/23694.

[13] Justo, J., Távara, L., García-Guzmán, L., and París, F. "Characterization of 3D printed long fibre reinforced composites", *Compos Struct*, vol. 185, pp. 537–548, Feb. 2018, doi: 10.1016/j.compstruct.2017.11.052.

[14] Ngo, T. D., Kashani, A., Imbalzano, G., Nguyen, K. T. Q., and Hui, D. "Additive manufacturing (3D printing): A review of materials, methods, applications and challenges", *Compos B Eng*, vol. 143, no. February, pp. 172–196, 2018, doi: 10.1016/j.compositesb.2018.02.012.

[15] Eiliat, H., and Urbanic, R. J. "Minimizing voids for a material extrusion-based process", *Rapid Prototyp J*, vol. 24, no. 2, pp. 485–500, 2018, doi: 10.1108/RPJ-05-2017-0092.

[16] Kishore, V. "Melt Processability and Post-Processing Treatment of High-Temperature Semi-Crystalline Thermoplastics for Extrusion Deposition Additive Manufacturing", pp. 1–127, 2018.

[17] Pascual-González, C. *et al.*, "Post-processing effects on microstructure, interlaminar and thermal properties of 3D printed continuous carbon fibre composites", *Compos B Eng*, vol. 210, no. November 2020, p. 108652, 2021, doi: 10.1016/j.compositesb.2021.108652.

[18] de Avila, E., Eo, J., Kim, J., and Kim, N. K. "Heat treatment effect on mechanical properties of 3D printed polymers", in *MATEC Web of Conferences*, EDP Sciences, 2019, pp. 1–5. doi: https://doi.org/10.1051/matecconf/2019264020 01.

[19] Guduru, K. K., and Srinivasu, G. "Effect of post-treatment on tensile properties of carbon reinforced PLA composite by 3D printing", *Mater Today Proc*, vol. 33, pp. 5403–5407, 2020, doi: 10.1016/j.matpr.2020.03.128.

[20] Meng, Q., Gu, Y., Luo, L., Wang, S., Li, M., and Zhang, Z. "Annealing effect on crystalline structure and mechanical properties in long glass fibre reinforced polyamide 66", *J Appl Polym Sci*, vol. 134, no. 23, pp. 1–10, 2017, doi: 10.1002/app.44832.

[21] Ivey, M., Melenka, G. W., Carey, J. P., and Ayranci, C. "Characterizing short-fiber-reinforced composites produced using additive manufacturing", *Advanced Manufacturing: Polymer and Composites Science*, vol. 3, no. 3, pp. 81–91, 2017, doi: 10.1080/20550340.2017. 1341125.

[22] Shiao, M. L., Nair, S. V., Garrett, P. D., and Pollard, R. E. "Effect of glass-fibre reinforcement and annealing on microstructure and mechanical behaviour of nylon 6 , 6 Part II Mechanical behaviour," *Journal of Material Science*, vol. 29, pp. 1739–1752, 1994, doi: 10.1007/BF00351291.

[23] Shiao, M. L., Nair, S. V., Garrett, P. D., and Pollard, R. E. "Effect of glass-fibre reinforcement and annealing on microstructure and mechanical behaviour of nylon 6,6 Part I : Microstructure and morphology", *Journal of material science*, vol. 29, pp. 1973–1981, 1994, doi: 10.1007/BF00351291.

[24] El Magri, A., El Mabrouk, K., Vaudreuil, S., and Ebn Touhami, M. "Mechanical properties of CF-reinforced PLA parts manufactured by fused deposition modelling," *Journal of Thermoplastic Composite Materials*, 2019, doi: 10.1177/0892705719847244.

[25] Bhandari, S., Lopez-Anido, R. A., and Gardner, D. J. "Enhancing the interlayer tensile strength of 3D printed short carbon fibre reinforced PETG and PLA composites via annealing," *Addit Manuf*, vol. 30, 2019, doi: 10.1016/j.ad dma.2019.100922.

[26] Hoang, V. T. *et al.*, "Postprocessing method-induced mechanical properties of carbon fibre-reinforced thermoplastic composites", *Journal of Thermoplastic Composite Materials*, 2020, doi: 10.1177/0892705720945376.

[27] Geng, P. *et al.*, "Effect of thermal processing and heat treatment condition on 3D printing PPS properties", *Polymers (Basel)*, vol. 10, no. 8, 2018, doi: 10.3390/polym10080875.

[28] Jain, P. J. A. K. "The Effect of Compaction Temperature and Pressure on Mechanical Properties of 3D Printed Short Glass Fiber Composites", *Master of Science, Old Dominion University*, 2020. doi: 10.25777/fghz-m472.